Probe diagnostic development for electron beam produced plasmas

D. D. Blackwell,[a),b)] S. G. Walton,[b)] D. Leonhardt, D. P. Murphy, R. F. Fernsler, W. E. Amatucci, and R. A. Meger
U.S. Naval Research Laboratory, Plasma Physics Division, Washington, DC 20375

(Received 9 October 2000; accepted 26 February 2001)

A variety of diagnostics have been fielded in different plasma sources to provide new information about the large area plasma processing system (LAPPS) at NRL. Specifically, a high resolution digital Langmuir probe system and ion flux/energy diagnostics have been employed in pulsed and dc electron beam produced plasmas as well as in an inductively coupled source as a baseline experiment. rf induced dc bias, ion flux, electron and ion temperature, and plasma potential in the proximity of rf powered electrodes placed into these plasmas were measured. It is found that the LAPPS plasma channel is essentially unaffected by the presence of the rf voltage, with the net ion flux unchanging in the presence of rf. These findings are consistent with earlier theoretical models of LAPPS [Manheimer *et al.*, Plasma Sources Sci. Technol. **9**, 370 (2000)]. © *2001 American Vacuum Society.* [DOI: 10.1116/1.1366699]

I. INTRODUCTION

Over the past few years at NRL there has been a considerable amount of experimental and theoretical effort put into producing and understanding electron beam plasmas.[1–3] One of the most unique features of electron beam produced plasmas is that the ionization is highly localized to the electron beam channel. Outside of this channel the plasma can be expected to rapidly diminish in both particle energy and density. Also, the high energy electron beam (>1 kV), and thus gas ionization, is unaffected by most other electric fields introduced artificially. These characteristics, in addition to the innate plasma uniformity along the beam axis, make these plasmas ideal for large surface processing applications. The ion flux and energy should be highly controllable, the electron temperature very low, and the flux area very large. The feasibility of using these sources depends in large part on how well the plasma follows these characteristics. Recently diagnostics have been developed at NRL capable of testing these expectations. In this article we present preliminary observations made with these diagnostics to verify and quantify some of the assumptions made about large area plasma processing system (LAPPS) operation.[4]

II. EXPERIMENT

A. Plasma source

Two electron beam plasma sources were used in the experiments. The first was a hollow cathode driven pulsed source. Details of this source are described elsewhere.[5] It produced 1 ms plasma pulses $1\times 20\,\mathrm{cm}^2$ in the $n_e \approx 10^{11}\,\mathrm{cm}^{-3}$ range in argon and oxygen. Figure 1 shows a diagram of the plasma source. A hollow cathode is affixed to one end of a 62 cm long by 55 cm diam aluminum cylinder. The cathode itself is simply a small (≈ 2 cm diam $\times 20$ cm long) hollowed out brass cylinder connected to the negative terminal of a high voltage power supply. The strong electric fields inside the hollowed out region break down the gas, and the electrons are driven to the grounded wall at the opposite end of the chamber. Two large magnetic field coils provide a magnetic field strength of 150 G which confines the hollow cathode produced plasma to a narrow slab. At the midpoint of the chamber and perpendicular to the magnetic field are two large (6 in. diam) access ports through which are inserted the various stages and diagnostics used.

The second source was a continuous current electron beam which created a $1\times 30\,\mathrm{cm}^2$ plasma in the $n_e \approx 5\times 10^{11}\,\mathrm{cm}^{-3}$ range. The plasma production method was slightly different in that the hollow cathode itself is operated at a relatively low voltage (300 V) and the beam is extracted into the chamber with a high voltage acceleration grid. In every other sense this source was virtually identical to the pulsed source.

B. Diagnostics

1. Langmuir probes

The Langmuir probes used were made from a 0.5 mm stock graphite rod and 1.5 mm alumina ceramic with 1 mm tips. Passive filtering was used to alleviate fluctuations in the plasma potential caused by the application of rf power to electrodes near the plasma according to the design outlined by Sudit and Chen.[6] High impedance Lenox–Fugle chokes at 13.56 and 27.12 MHz and a secondary probe which was connected to the primary collecting probe through a 10 nF capacitor were used to reduce the rf voltage drop across the probe sheath.

The probes are swept with a programmable power supply and the current signal obtained from the differential voltage across a sampling resistor. The signals are fed into a CAMAC digitizer and subsequently recorded. The probe data is twice differentiated using a Savitsky–Golay smoothing window which gives the energy distribution function from the Druyvesteyn formula

[a)]Electronic mail: davidb@ccs.nrl.navy.mil
[b)]NRL/NRC postdoctoral research associate.

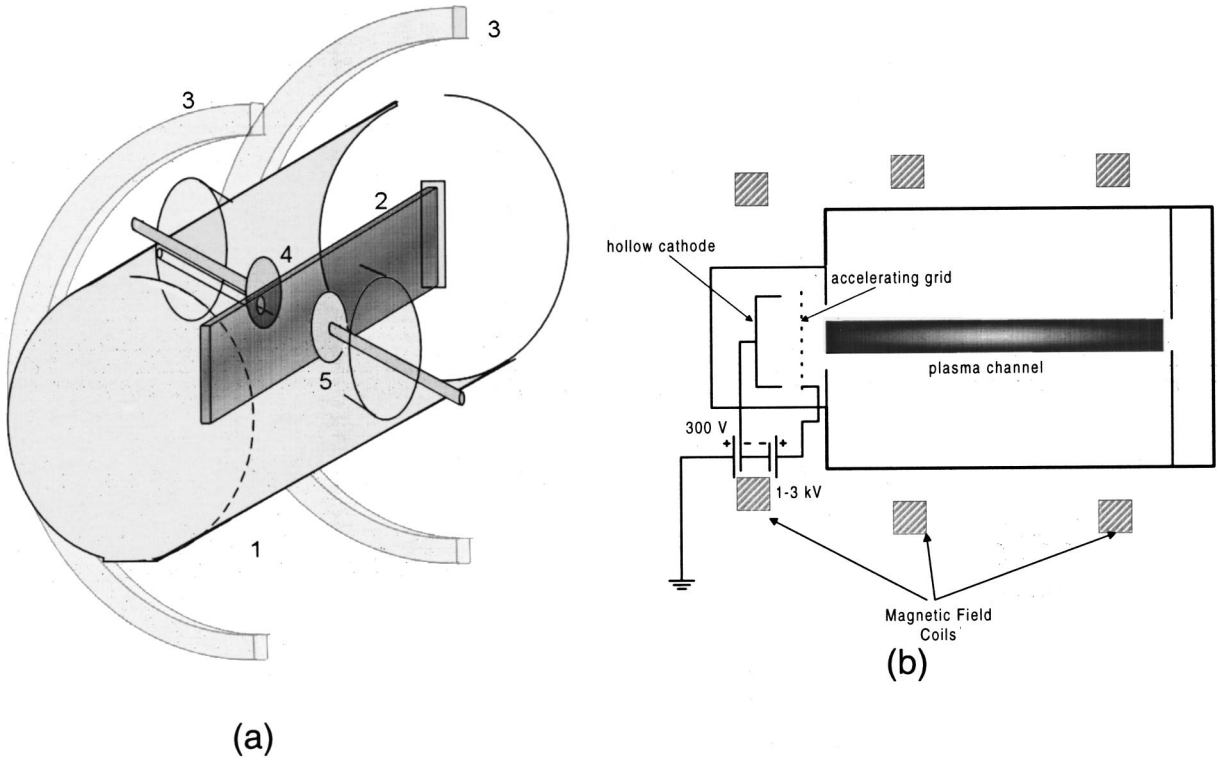

FIG. 1. (a) Illustration of the chamber and experimental section of the pulsed and continuous cathode sources. (1) 62×55 cm aluminum chamber. (2) Plasma sheet. (3) Magnetic field coils. (4) Diagnostic feedthrough, shown with ground plane and Langmuir probe setup. (5) rf stage feedthrough, shown with 2.5 in. diam rf driven electrode. (b) Schematic of hollow cathode setup for the contiuous current source.

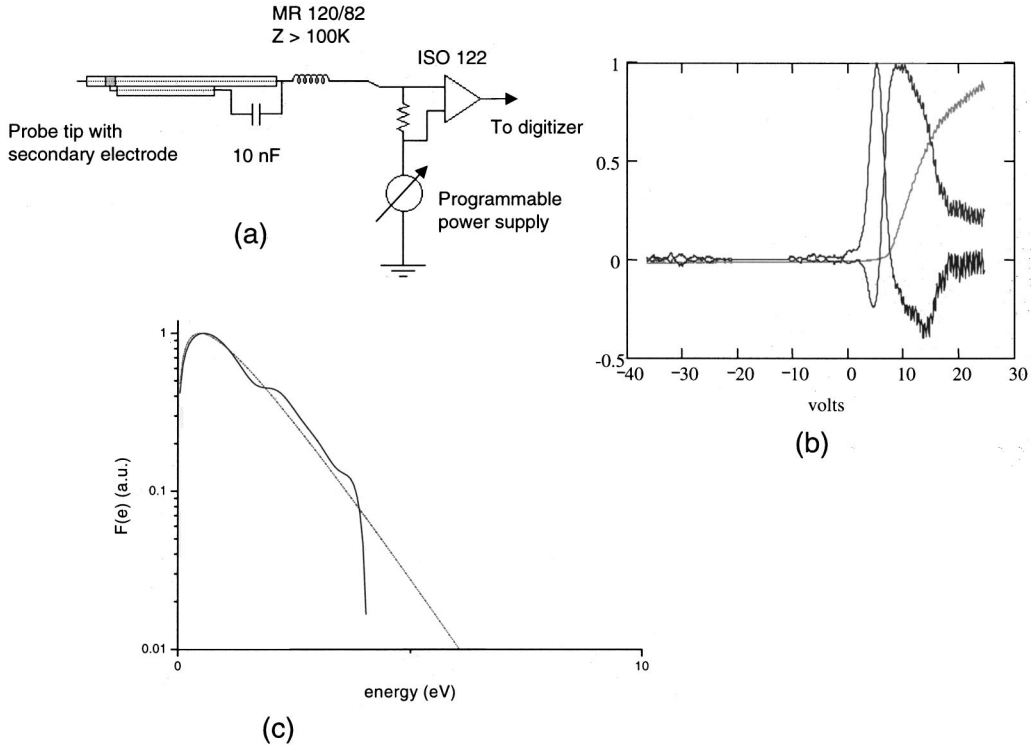

FIG. 2. (a) Probe circuit setup and (b) resulting characteristic, shown with first and second derivatives. (c) The EEDF calculated from Eq. (1). The probe characteristics were taken in the central plasma channel from the continuous current plasma source under typical conditions of 1 kV cathode voltage, 250 G magnetic field, and 50 mT argon. For comparison purposes a 1 eV Maxwellian is shown as the dashed line over the range for which this curve could be reliably resolved.

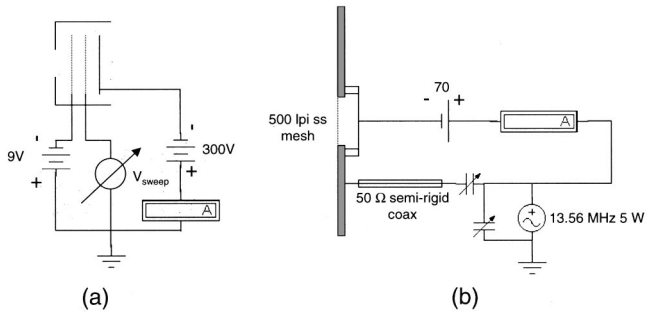

FIG. 3. (a) Gridded ion energy analyzer and (b) the rf stage mounted flux collector.

$$F[e(V_p-V_B)]=\frac{4}{Ae^2}\sqrt{\frac{mV_p-V_B)}{2e}}\frac{d^2I}{dV_B^2}, \tag{1}$$

where A is the probe area, V_p the plasma potential, and V_B the probe bias voltage. A diagram of the probe circuit setup and an example of the probe signals and derivatives are shown in Fig. 2. More details concerning the probe data acquisition and analysis will be presented in a future paper.

2. Ion flux diagnostics

Two types of ion flux collectors were used in the experiments. The first was a gridded analyzer with a 0.5 in. diam body mounted on a 0.375 in. shaft. A 0.25 in. opening admits ions to a 500 lpi mesh biased at −9 V. The ions which pass through this mesh encounter a second screen which is biased with a sweepable voltage. Whatever ions get through are then collected by a collector placed behind this biased at −300 V. This high negative collector bias helps suppress any secondary emission or other stray electrons. The current signal from this collector can then be differentiated to give the ion energy distribution as

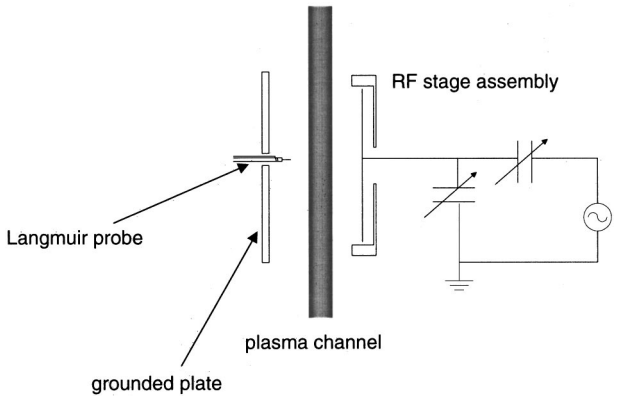

FIG. 4. Experimental setup for Langmuir probe measurements in the plasma channel.

$$F(v_\parallel)\propto\left[\frac{dI}{dV}\right]_{eV=1/2mv_\parallel^2} \tag{2}$$

with

$$F(v_\parallel)=\int_{-\infty}^{\infty}\int_{-\infty}^{\infty}f(v_\parallel,\mathbf{v}_\perp)d\mathbf{v}_\perp .$$

Here $v_\parallel$ and $v_\perp$ are the velocity components parallel and perpendicular to the discriminator grid normal. It is clear from Eq. (2) that for an isotropic ion distribution this represents the actual energy distribution $F(e)$.

The second flux diagnostic was a negatively biased collector incorporated into a rf powered electrode to monitor incident ion flux. A 0.25 in. hole covered with a 500 lpi screen admits ions to a 0.125 in. disk biased at −70 V. Figure 3 shows both types of ion flux probes.

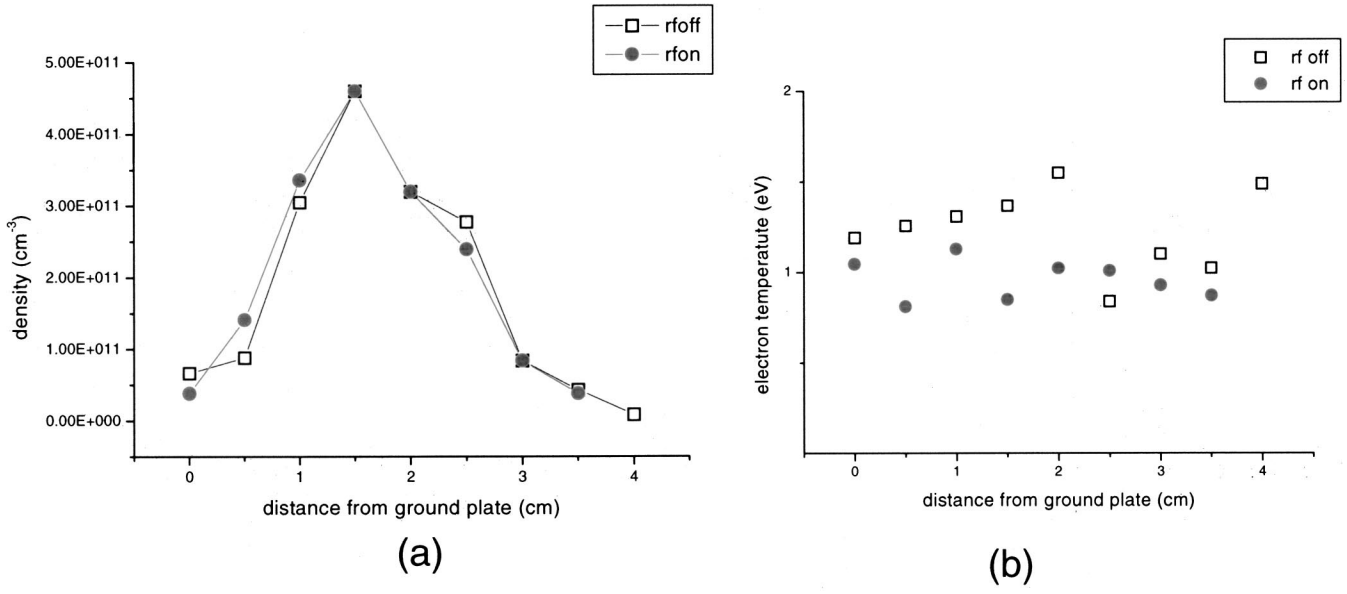

FIG. 5. Electron density (a) and temperature (b) derived from the EEDF in the plasma channel. The beam energy is 1 kV, the magnetic field 250 G, and the argon pressure 50 mTorr.

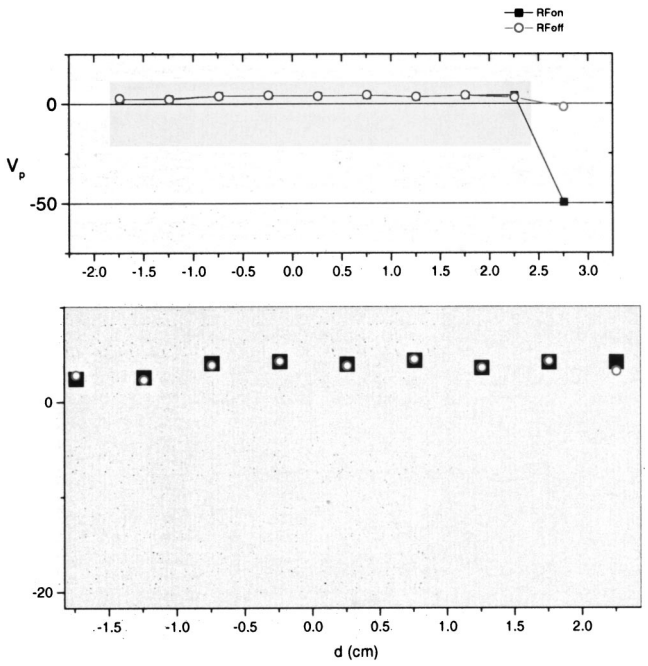

FIG. 6. Plasma potential with and without rf applied to the electrode in the contiuous current source. A strong negative bias is induced on the electrode by the rf voltage without affecting the plasma potential in the channel region.

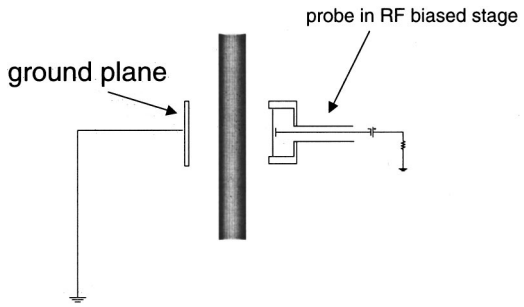

FIG. 7. Experimental setup for measuring the ion flux to a rf biased stage.

III. RESULTS

A. Plasma channel probe measurements

The small sized Langmuir probes were the diagnostics of choice for measurements done within the LAPPS plasma channel. A 2.5 in. rf biased electrode was positioned 4 cm from the edge of the plasma channel. The probe was inserted from the side opposite the rf stage through a 2.5 in. grounded electrode also located 4 cm from the plasma. A diagram of this setup is shown in Fig. 4.

Figures 5 and 6 are plots of the electron density, temperature, and plasma potential from a 1 kV beam in 50 mTorr argon and a 250 G magnetic field in the continuous plasma source. The rf electrode had 5 W of 13.56 MHz power applied to it which gave rise to a peak-to-peak voltage of 170 V and a self-induced dc bias of −70 V. The plasma density and temperature are unchanged with the application of this rf voltage applied to the plate. We can see that the potential profile is fairly flat between the two electrodes while the density has a full width at half maximum of ≈2 cm. The exception to this is when rf power is applied to the powered electrode; here the potential is forced to steeply drop within 5 mm to the value of the induced bias. These measurements demonstrate decoupling of the plasma production mechanism from the electrode conditions. All measurements inside the channel were unaffected by the presence (or lack thereof) of rf power to the electrode, while a large sheath voltage drop was still provided.

B. Ion flux measurements

Figure 7 shows the experimental setup for the flux measurements in the continuous source. As the stage is moved towards the sheet of plasma, the flux is recorded with the rf power on, off, and with the rf power on but the electron beam turned off. Figure 8 is a plot of the flux measurements with beam energies of 1.25 and 2.5 kV and a magnetic field of 250 G. Figure 9 shows the corresponding rf voltage and self-bias voltage on the electrode at each condition. From these plots we see that the presence of the beam plasma

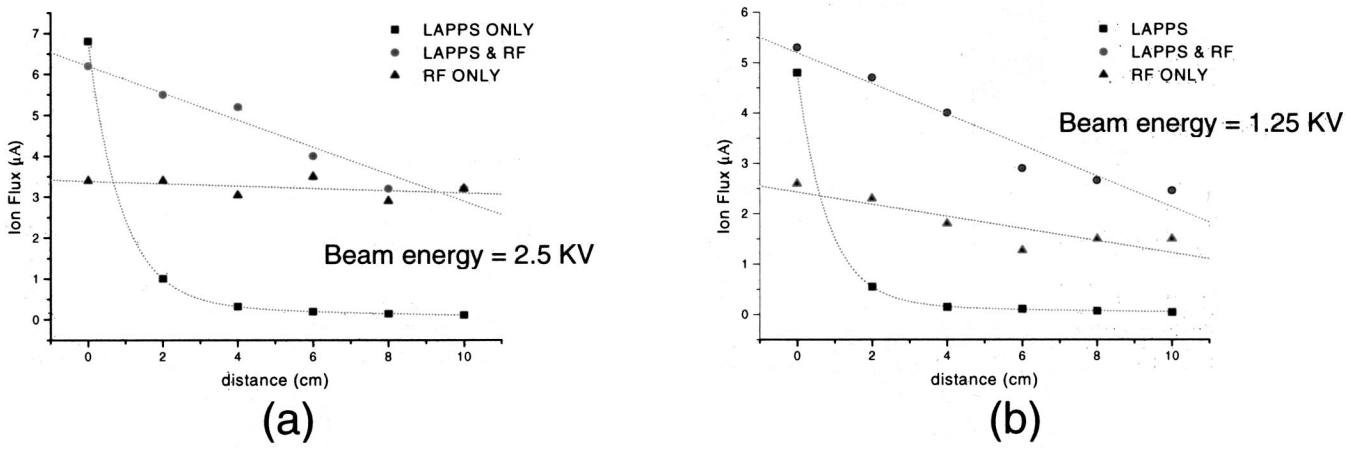

FIG. 8. Ion flux vs radial distance from the edge of the plasma sheet defined as the axial projection of the cathode slot opening in the continuous current source. The cathode voltage is set to (a) 2.5 kV and (b) 1.25 kV with a magnetic field of 250 G and argon pressure of 50 mTorr.

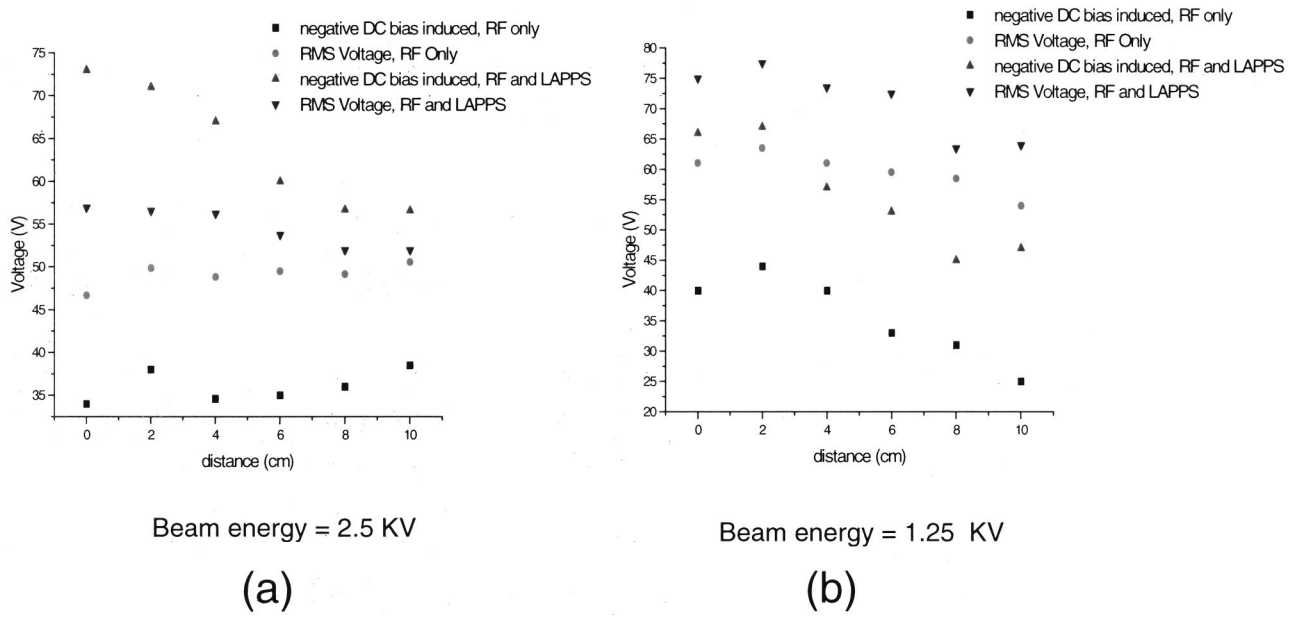
negative DC bias induced, RF only
RMS Voltage, RF Only
negative DC bias induced, RF and LAPPS
RMS Voltage, RF and LAPPS
Voltage (V)
distance (cm)
Beam energy = 2.5 KV
(a)
negative DC bias induced, RF only
RMS Voltage, RF Only
negative DC bias induced, RF and LAPPS
RMS Voltage, RF and LAPPS
Voltage (V)
distance (cm)
Beam energy = 1.25 KV
(b)

FIG. 9. rf voltage and induced negative dc bias under the conditions described in Fig. 8.

causes an increase in the self-bias and a decrease in the rf voltage required to achieve that bias with the same amount of rf power applied (5 W). In the vicinity of the LAPPS channel, applying rf power alone creates a weaker plasma and lower flux than applying it when the LAPPS plasma is running. The converse of this is not true, however. The flux from LAPPS alone and the flux from LAPPS when the rf is on are identical within experimental error. The only function of the rf is to accelerate ions to the electrode. The flux from LAPPS also decreases very quickly with distance from the channel, most probably due to recombination and charge exchange of the ions.

The ion energy measurements are carried out in the pulsed hollow cathode source. The setup is identical to Fig. 7 except the rf stage mounted flux collector of Fig. 3(b) is replaced by the analyzer of Fig. 3(a). A boxcar averager was used to extract the ion characteristic by sweeping the discriminator grid voltage over successive pulses. The source was operated with either 30 mTorr of argon or oxygen in a 150 G magnetic field and a beam energy of 2 kV. As shown in Fig. 10 the typical ion energy distribution derived from Eq. (2) was Gaussian, which is consistent with Ref. 7. The table in Fig. 10 shows that the effective ion temperature defined as

$$T_{\text{eff}} = \frac{2}{3}\frac{\int_0^\infty e f(e)de}{\int_0^\infty f(e)de}$$

appears to increase at a greater distance from the plasma channel. This is likely due to higher incidence of collisions in the sheath as the plasma density drops. This is because the main ion collision mechanism, ion-neutral collisions, remains unchanged while the lower density makes the sheath region thicker. As expected, the lower electron temperature oxygen plasma produces lower temperature ions.[8,9] In all cases the distribution is centered near the plasma potential within reasonable error.

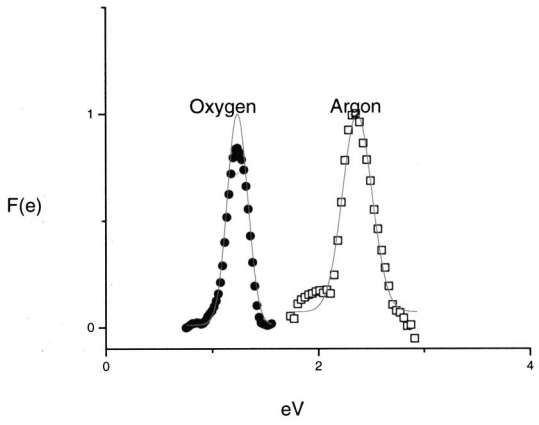

Distance from plasma edge	0.5 cm	1.5 cm
Teff (Oxygen)	0.1	0.05
Teff (Argon)	0.09	0.14

FIG. 10. Ion energy distributions in argon and oxygen at 30 mTorr with a magnetic field of 150 G and a 2 kV cathode in the pulsed cathode source.

IV. SUMMARY

The measurements presented in this article demonstrate that beam produced plasmas behave as expected with characteristics well-suited to processing applications. The ion energy is controllable by applying rf power to the surface

to be treated, with very small ion and electron temperatures. The source is very well decoupled from the processing stage. Future work will combine the two ion flux diagnostics to give an account of ion energy to a rf powered electrode.

ACKNOWLEDGMENTS

This work was supported by the Office of Naval Research. D. D. Blackwell and S. G. Walton thank the National Research Council for their support.

[1]R. F. Fernsler, W. M. Manheimer, R. A. Meger, J. Mathew, D. P. Murphy, R. E. Pechacek, and J. A. Gregor, Phys. Plasmas **5**, 2137 (1998).
[2]J. Mathew, R. F. Fernsler, R. A. Meger, J. A. Gregor, D. P. Murphy, R. E. Pechacek, and W. M. Manheimer, Phys. Rev. Lett. **77**, 1982 (1996).
[3]R. A. Meger, J. Mathew, J. A. Gregor, R. E. Pechacek, R. F. Fernsler, W. M. Manheimer, and A. E. Robson, Phys. Plasmas **2**, 2532 (1995).
[4]W. M. Manheimer, R. F. Fernsler, M. Lampe, and R. A. Meger, Plasma Sources Sci. Technol. **9**, 370 (2000).
[5]See D. Leonhardt *et al.*, J. Vac. Sci. Technol. A, these proceedings.
[6]I. D. Sudit and F. F. Chen, Plasma Sources Sci. Technol. **3**, 162 (1994).
[7]See S. G. Walton *et al.*, J. Vac. Sci. Technol. A, these proceedings.
[8]R. D. Hake and A. V. Phelps, Phys. Rev. **158**, 70 (1967).
[9]W. P. Allis and H. A. Haus, J. Appl. Phys. **45**, 781 (1974).